Time Irreversibility of Cycle-by-Cycle Engine Combustion Variations

J.B. Green, Jr.,* C.S. Daw, J.S. Armfield
Oak Ridge National Laboratory
Oak Ridge TN 37831-8087

C.E.A. Finney
University of Tennessee
Knoxville TN 37996-2210

P. Durbetaki
Georgia Institute of Technology
Atlanta GA 30332-0405

Abstract

Spark-ignition engines exhibit patterns of increasing instability as engine fueling goes from stoichiometric to lean. The observation of time irreversibility in cycle-resolved combustion measurements indicates that this combustion instability is inherently nonlinear. Using time return maps and symbolic time-series analysis, we demonstrate the presence of strong time irreversibility in experimental data from production and laboratory spark-ignition engines under lean fueling. We propose that the time-irreversible patterns can be explained as the result of nonlinear coupling between successive cycles combined with the effects of dynamic noise. This model is inherently distinct from models which attempt to explain cyclic variations as arising from linear Gaussian random processes.

Introduction

Cyclic combustion variability is a phenomenon that has been studied and continually debated for almost 100 years. Explanations for the basic causes have ranged from random in-cylinder mixing processes to deterministic coupling between cycles (the so-called prior-cycle effect). The most recent version of the deterministic-coupling model is based on concepts from nonlinear dynamics and chaos theory [1,2,3,4]. Whatever their source, these combustion oscillations are responsible for higher emissions of both nitrogen oxides and unburned hydrocarbons. A better understanding of the basic causes of cyclic variations could potentially provide a means for extending the practical lean limit of spark-ignition engines and improving emissions control and fuel efficiency.

Two of the most prominent explanations for the deterministic character seen in cyclic variations in spark-ignition engines operating at very lean conditions are summarized by the linear Gaussian random process model (LGRP) and the noisy nonlinear dynamics model (NND). The first model (LGRP) is based on the assumption that cyclic combustion variations arise from linearly correlated fluctuations in the as-injected air/fuel ratio. Such fluctuations could be caused by acoustic modes excited by flow turbulence. Because flame propagation is nonlinearly affected by small fluctuations in air/fuel ratio near the lean limit, the as-injected fluctuations would tend to be amplified to produce large combustion variations. However, these variations would be dominated by intake effects; thus the engine would simply follow the linear dynamics of the intake system. There is no "memory" of past combustion events passed to the future.

The NND model assumes that the dominant mechanism of combustion instability is residual gas. Specifically, residual fuel and air left from past combustion events are assumed to mix with freshly injected fuel and air, and the resulting mixture then burns. Like the LGRP model, small changes in fuel/air ratio at the time of spark can cause wide variations in combustion. However, unlike the LGRP model, the combustion is directly affected by the strength of previous combustion events. This type of nonlinear "memory" can produce much more interesting and complex behavior, most notably bifurcations and chaos.

Recent work in dynamic systems theory has shown that one critical feature which can be used to discriminate models like the above is time irreversibility [5]. Specifically, processes consistent with LGRP do not exhibit an arrow of time — their behavior in forward time appears statistically the same with their behavior when time is reversed (or we look at the behavior with time running backwards). Processes consistent with NND, however, have a definite arrow of time which increases in importance as the nonlinear "memory" is increased. Thus it would be extremely helpful to have measures of time irreversibility to use in evaluating which of the two models better explains observations of cyclic combustion variations.

In the following discussion we describe proposed methods for evaluating time irreversibility in cyclic com-

* Corresponding author

bustion measurements. We also describe our experimental measurement procedures and illustrate results for data from two different types of spark-ignition engines.

Experimental apparatus and methods

The first experimental engine was a production in-line four-cylinder port-fuel-injected engine (General Motors Quad4). The engine has a 2.3-L displacement, 9.2-cm bore, 8.5-cm stroke and compression ratio of 9.5. The nominal engine operating condition was 1200 RPM and 40 CAD before top center spark. An absorbing dynamometer was operated in speed-control mode to maintain engine speed. Data sets were generated at injected equivalence ratios of 0.99, 0.78 and 0.73. All other feedback controllers were disabled, and the engine was run in open-loop mode, except for dynamometer speed control. This strategy assured that combustion was minimally influenced by feedback controllers while the engine ran at a nominal engine speed.

The second experimental engine system was a single-cylinder spark-ignited, L-head engine (Kohler Magnum 12). The engine has a 0.476-L displacement, 8.59-cm bore, 8.26-cm stroke and compression ratio of 6.6. A motoring dynamometer was used to maintain a nearly constant engine speed of 1200 RPM, and spark timing was maintained at 40 CAD before top center. Data sets were generated at injected equivalence ratios of 0.99, 0.77 and 0.73. The engine was run in open-loop mode and all other engine controls were disabled to minimize the effect of these controls on cycle-by-cycle engine dynamics.

Both engines are equipped with an electronic engine management system that controls fuel injection and regulates spark timing. A PC-based data-acquisition system was used to acquire high- and low-speed engine operating and performance data during testing. Combustion pressure was recorded once per CAD from a single cylinder for over 3000 contiguous cycles. The fuel used in all experiments was indolene. Combustion pressure measurements were made with a piezoelectric pressure transducer. To provide a dynamic measurement that could be compared with the model, the combustion heat release for each cycle was calculated by integrating the cylinder pressure data using a technique equivalent to the Rassweiler-Withrow method [6,7]. As a result, for each engine experiment a time series of over 3000 heat-release values was produced.

Return maps

Time reversibility is defined such that a qualitative or quantitative description of a time series is indistinguishable from a time-reversed version of itself. Time return maps provide a simple way to determine qualitatively whether time reversibility is present in engine data. Figure 1 illustrates this with return maps of cycle resolved heat release for the Kohler engine. Return maps plot each successive pair of heat release values (that is, the heat releases for every cycle i and cycle i+1) as points in a plane. With each new cycle, the current point "maps" into the next, building up a composite statistical picture of how cycles are interrelated.

As shown in Fig. 1(a–c), the character of the return maps for the Kohler engine changes drastically as the fueling becomes increasingly lean. At near stoichiometric fueling, the points collect in a "shotgun" pattern near a central point and the range of heat release variability is relatively small. As fueling is leaned, the onset of engine stability produces occasional misfires that create large excursions away from the central region. The excursions become larger as the engine is operated even leaner, and characteristic "arms" emerge in the collective plots of many successive cycles. Multiple sequential misfires at very lean fueling produce flat regions near the ends of the arms.

One characteristic of the return maps here which is particularly relevant to the question of time irreversibility is the emergence of asymmetry about the diagonal. With examination, it becomes clear that the patterns in (b) and (c) are skewed in their distributions about the diagonal. This can be readily seen by comparison of these plots with those on in (e) and (f). In these latter plots the (i) and (i+1) axes have been reversed, reflecting the change that is produced when the flow of time is reversed. Particular asymmetric features to note are the second vertical band of points to the right of the diagonal in (b) and (c) and the displacement of the "vertex" of the arms to the right as fueling is leaned.

From the above observations, we see immediately that time irreversible characteristics seem to emerge and get more pronounced as fueling is leaned. As we discuss in the following sections, it is possible to more quantitatively describe the strength of this asymmetry and to use it to compare the relative agreement between the two proposed cyclic variability models and our experimental heat release data.

Symbolization

For more quantitative evaluations of time irreversibility in engine heat-release measurements, we employ an approach known as symbolic time-series analysis or symbolization for short. The symbolization methods we describe here are based on the general approach suggested by Tang *et al.* [8] with some modifications to address time irreversibility. For more detailed information on the theoretical basis and development of symbolization as a data-analysis tool, the reader is referred to [9,10].

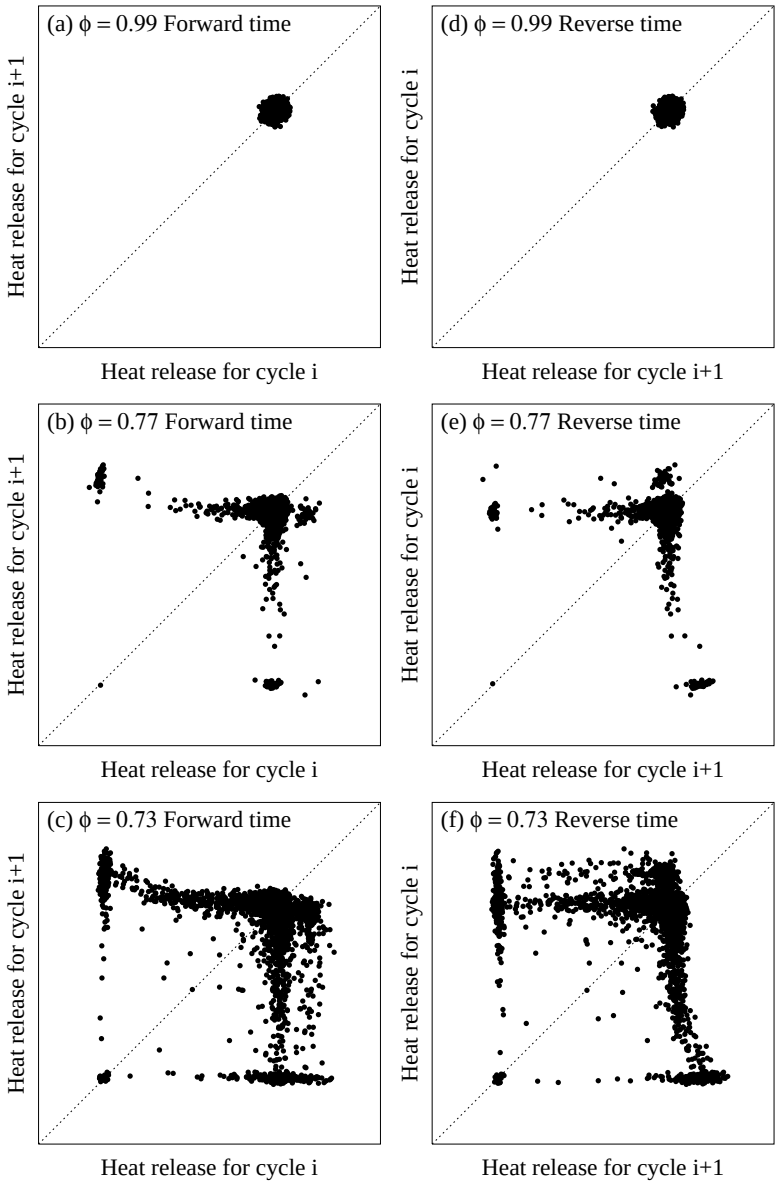

Figure 1: Time return maps for the Kohler engine at equivalence ratios of 0.99 (a,d), 0.77 (b,e) and 0.73 (c,f).

The key step in applying symbolization to time-series measurements involves transforming the original values into a stream of discretized symbols. We accomplish this by partitioning the range of the observed values into a finite number of regions (usually less than 10) and then assigning a symbol to each measurement based on which region it falls into. For example, the simplest scheme is to assign values of 0 or 1 to each observation depending on whether it is above or below some critical value (a so-called binary partition). More partitions yield larger "alphabets" of symbols, one symbol for each discrete region of the data range. For the results presented here, we define our partitions such that the individual occurrence of each symbol is equiprobable (that is, the likelihood of observing a single measurement in any given region is the same).

Once a time series is symbolized, the relative frequencies of all possible sequences of length L in the data provide a fast and efficient way to characterize temporal patterns. A simple way to create symbol-sequence histograms is to assign a unique number that identifies each possible sequence, thus making it possible to plot frequency versus symbol number to depict the relative frequency for each pattern. We assign a sequence "code" to each pattern by using the equivalent base-10 value of each base-n sequence, where n is the number of parti-

tions. For example, a symbol sequence of 1 0 1 for a binary partition would have a sequence code of 5. Because of our equiprobable partitioning convention, the relative frequency of each sequence for random data will be equal (subject to sampling fluctuations). Thus any significant deviation from equiprobable sequences is indicative of time correlation and determinism.

Symbol-sequence histograms are very useful for quantifying time irreversibility because the relative frequencies will shift when the data are observed in backwards time. Conversely, if the process being measured is time symmetric, then we should see no significant change in the histogram when it is constructed in backwards time. To compare forward- and reverse-time histograms, we use a Euclidean norm statistic defined by

$$\Delta_{AB}(L) = \sqrt{\sum_i (A_{i,L} - B_{i,L})^2} \ , \qquad (1)$$

where i is indexed over all possible sequence codes. A and B in the above equation are the histogram frequencies for the forward- and reverse-time analyses, respectively. The magnitude of Δ indicates the difference between the two histograms and thus quantifies the level of time irreversibility.

Figure 2 illustrates symbol-sequence histograms for the forward- and reverse-time realizations of data from the Quad 4 engine. The assumed symbolization parameters in this case are an 8-level symbolization (8 possible symbols) and a sequence length of 2 cycles. Thus there are 8^2 or 64 possible sequences to account for. Moving down the column of plots from (a) to (c), we see the change in behavior associated with reducing the as-injected equivalence ratio ϕ from 0.99 to 0.78 to 0.73. In (a), we see that both the forward- and reverse-time realizations are essentially flat (except for random fluctuations) and are very similar (implying no significant time asymmetry). In (b) and (c), however, we see that major peaks have developed and that these peaks are very different for the forward- and reverse-time realizations. Thus it is clear that time irreversibility has emerged with leaner fueling.

From a physical perspective, the large peak on the left end of Fig. 2 represents the occurrence of a misfire/energetic-burn sequence (i.e., a 0 7 sequence), while the energetic-burn/misfire sequence is represented by the much smaller peak (7 0) on the right-hand side of the plot (in forward time). The large difference in amplitude between these peaks suggests that there is s strong preference for the order in which they occur. As we describe in the next section, this preference for order has important implications for selecting the best model of cyclic variation.

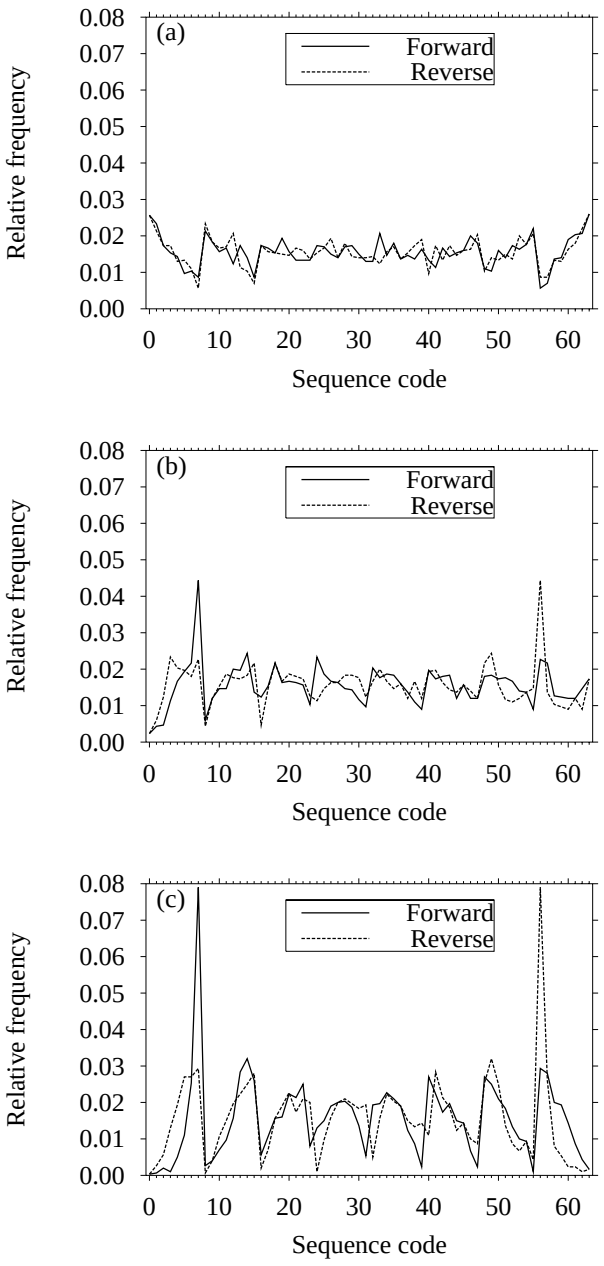

Figure 2: Symbol-sequence histograms of heat release in forward- and reverse-time for the Quad4 engine at equivalence ratios of 0.99 (a), 0.78 (b) and 0.73 (c).

Model discrimination

As previously discussed, two prominent approaches that have been proposed to explain lean-fueling cyclic variations are the linear Gaussian random process model (LGRP) and the noisy nonlinear dynamics model (NND). The LGRP model attributes the dominant cause of cyclic variations to be linear oscillations in the intake system ex-

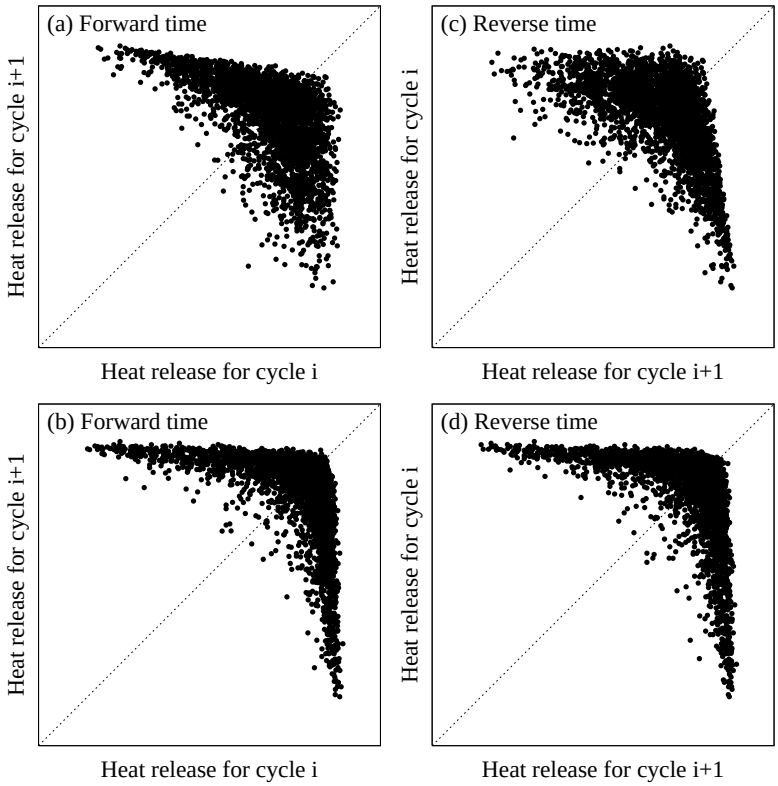

Figure 3: Time return maps for NND model in forward (a) and reverse (c) time and LGRP model in forward (b) and reverse (d) time.

cited by Gaussian random noise, and the NND model attributes the dominant cause to nonlinear coupling between cycles through residual gas. Even though the deterministic effects in the LGRP model are driven by linearly correlated fuel fluctuations, the nonlinear amplification caused by the combustion process makes the dynamic behavior pseudo-nonlinear. However, the LGRP model cannot exhibit bifurcations and chaos, a prominent feature of the NND model. These models are also very different in that the LGRP model cannot produce time irreversibility but the NND model can. If we start with a null hypothesis that the primary cause of cyclic variations are due to either one or the other of these models, we can use time irreversibility to test which hypothesis is correct.

To compare the models with each other and our data, we generated 3000 simulated heat-release values from the version of the NND model presented by Daw *et al.* [1] and a modified version of the Daw *et al.* model which met the LGRP requirements. Specifically, the Daw *et al.* model predicts the heat-release output from sequential engine cycles by accounting for fuel and air balances and the nonlinear effect of equivalence ratio on combustion near the lean limit. Gaussian noise is also assumed to perturb the as-injected equivalence ratio reflecting the complex processes associated with air-fuel mixing and fuel droplet evaporation. For NND simulation with the Daw *et al.* model, we used residual-gas fractions between 5 and 30 percent. For LGRP simulation, we set the residual fraction to zero and added an anti-correlated linear filter so that the noisy perturbations to ϕ were anti-correlated from one cycle to the next. Anti-correlation was needed to produce the typical oscillating effect (misfire/energetic burn) seen in engines at lean fueling.

The results of our model simulations for lean fueling were then compared using time return maps and symbol-sequence histograms. As shown in Figure 3, both models reproduced certain features we observe experimentally at lean fueling. For example, the global patterns for both have a characteristic "crescent" shape opening to the left. However, on closer examination, we see that the NND return map exhibits a definite asymmetry about the diagonal, while the LGRP return map appears at least qualitatively symmetric.

We compared the models more rigorously using symbolization. Figure 4 illustrates the symbol-sequence histogram differences for forward- and reverse-time realizations of both model outputs. Note that the forward and reverse histograms for the LGRP model are virtually in-

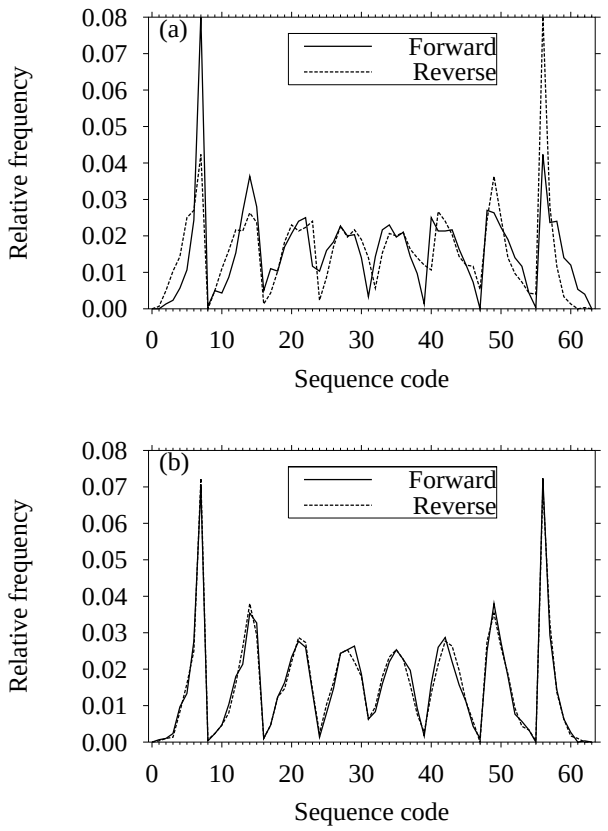

Figure 4: Symbol-sequence histograms of forward- and reverse-time NND model (a) and LGRP model (b) data.

distinguishable, but the histograms for the NND model are totally different. Using 200 simulation runs of 3000 cycles for each model, we further estimated the Δ statistic as defined by Eqn. 1 for each run. From the average and standard deviation of these values we determined that the Δ statistic for the LGRP model is 0.0186 ± 0.008 with 99% confidence and for the NND model it is 0.0898 ± 0.0126. The Δ statistic for the Quad4 engine data depicted in Fig. 2(c) is 0.0881, making it much more likely to be consistent with the NND model.

Conclusions

From the above results, we see that symbol statistics and time irreversibility can play an important role in discriminating between engine models for cyclic dispersion. In the future, we intend to use this feature to improve the accuracy of the Daw *et al.* model.

References

1. Daw C.S., Finney C.E.A., Green J.B. Jr., Kennel M.B., Thomas J.F., Connolly F.T. (1996). "A simple model for cyclic variations in a spark-ignition engine", SAE Paper No. 962086.
2. Letellier C., Meunier-Guttin-Cluzel S., Gouesbet G., Neveu F., Duverger T., Cousyn B. (1997). "Use of the nonlinear dynamical system theory to study cycle-to-cycle variations from spark-ignition engine pressure data", SAE Paper No. 971640.
3. Daw C.S., Finney C.E.A., Kennel M.B., Connolly F.T. (1997). "Cycle-by-cycle variations in spark-ignited engines", *Proceedings of the Fourth Experimental Chaos Conference*.
4. Wagner R.M., Drallmeier J.A., Daw C.S. (1998). "Prior-cycle effects in lean spark ignition combustion: fuel/air charge considerations", SAE Paper No. 981047.
5. Diks C., Houwelingen J.C. van, Takens F., DeGoede J. (1995). "Reversibility as a criterion for discriminating time series", *Physics Letters A* **201**, 221–228.
6. Grimm B.M., Johnson R.T. (1990). "Review of simple heat release computations", SAE Paper No. 900445.
7. Heywood J.B. (1988). **Internal Combustion Engine Fundamentals**, McGraw-Hill, ISBN 0-07-028637-X.
8. Tang X.Z., Tracy E.R., Boozer A.D., deBrauw A., Brown R. (1995). "Symbol sequence statistics in noisy chaotic signal reconstruction", *Physical Review E* **51**:5, 3871–3889.
9. Finney C.E.A., Green J.B. Jr., Daw C.S. (1998). "Symbolic time-series analysis of engine combustion measurements", SAE Paper No. 980624.
10. Daw C.S., Kennel M.B., Finney C.E.A., Connolly F.T. (1998). "Observing and modeling nonlinear dynamics in an internal combustion engine", *Physical Review E* **57**:3, 2811–2819.